November 20th, 2017
Primary Author: Jingjie Zheng

Investigation of Crystal Structures using X-Ray Diffraction

Jingjie Zheng and Deepak Sathyan
Advanced Laboratory, Physics Department, College of Arts and Sciences, Boston University, Boston, MA 02215, USA
(Dated: November 20th, 2017)

X-ray crystallography is a technique that uses X-ray diffraction to investigate structures of molecules and crystals. This paper describes an experiment aiming to utilize this technique. An X-ray spectrometer was used to produced X-ray and create diffraction patterns. After interpreting these patterns, we measured the lattice constant of lithium fluoride (LiF) to be $403\ \text{pm} \pm 5\ \text{pm}$, and measured the lattice constant of potassium chloride (KCl) to be $622\ \text{pm} \pm 9\ \text{pm}$.

I. INTRODUCTION

X-rays are high energy electromagnetic waves that have wavelengths ranging from 10 pm to 10 nm, which is of the order of atomic spacings in molecules and crystal lattices. Wilhelm Röntgen, a German mechanical engineer and physicist, discovered X-ray on November 8th, 1895, which earned him the first Nobel Prize in Physics in 1901. [1]

Since then, the application of X-ray has led to many significant discoveries, including the establishment of the field of X-ray crystallography by William Henry Bragg and William Lawrence Bragg. [2] As the founders of the field, they invented the X-ray spectrometer, and by producing and interpreting X-ray diffraction patterns, they were able to analyze atomic and molecular structure of crystals and molecules. Due to this use, X-ray crystallography has made many important contributions in the fields material science, chemistry, and biology. [3]

Our experiment, as detailed in this paper, aimed to investigate the crystal structures of lithium fluoride (LiF) and potassium chloride (KCl) by interpreting X-ray diffraction patterns. This was achieved by producing X-ray using an X-ray tube, shining the X-ray on the surface of the underlying crystal at a certain incident angle, and measuring the intensity of the diffracted X-ray.

II. THEORY

The X-rays are produced by an X-ray tube with the mechanism as discussed below. In the tube, a metal filament is first heated by a low voltage current, thereby releasing a stream of electrons through thermionic emissions. The emitted electrons are linearly accelerated by an applied electric field in the vacuum and travel toward a metal target, or a piece of copper (Cu) in our experiment. As these high energy particles hit the copper target, X-rays are produced in two ways. In the first way, X-rays are emitted as the electrons are decelerated according to Maxwell's equations in classical electromagnetism. X-rays produced in this way are called bremsstrahlung. In the second way, copper atoms in the metal target are excited and ionized by the incoming electrons. Electrons that are originally in the innermost atomic shells (K shells) transit into upper shells in this excitation, leaving K shells unoccupied. Then, to fill this gap in the K shells, electrons in upper level shells transit down and simultaneously emit X-ray photons. Each of these X-ray photons has energy that equal to the energy level difference between upper and lower shells. These X-rays, as produced in Cu atoms, are called characteristic X-rays of Cu atoms. We produced mostly two types of characteristic X-rays in our experiment, K_α and K_β, which correspond to two different levels of electron transitions, as shown in Figure 1. Among the spectrum of the X-ray being produced, K_α X-rays have the highest intensity following by K_β X-rays. X-rays with other wavelengths, including bremsstrahlung, are also produced but with intensities relatively lower than K_α and K_β.

The emitted X-rays incident the surface of the crystal at an angle, θ, as shown in Figure 2. After being scattered by anions and cations in the crystal, the X-rays interfere with

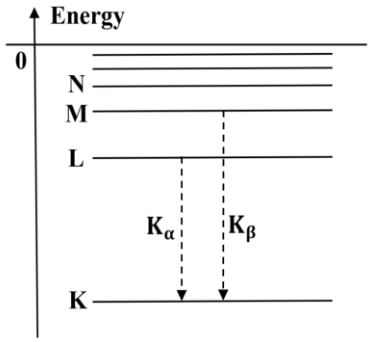

FIG. 1. Electron transitions from high energy levels to lower energy levels. K_α characteristic X-rays are produced by transitions from L shell to K shell. K_β characteristic X-rays are produced by transitions from M shell to K shell.

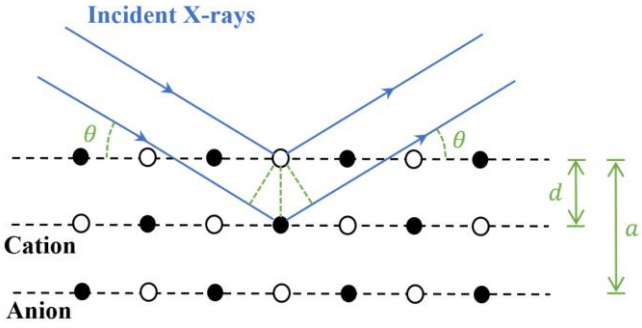

FIG. 2. An illustration of X-ray diffraction and Bragg's law.

one another destructively. However, at a certain angle, θ, and for a certain wavelength, λ, of the incident X-ray, constructive interference of the diffracted X-rays can be formed and detected. In order to establish such X-ray diffraction patterns, the following condition needs to be satisfied according to Bragg's law:

$$n\,\lambda = 2\,d\,\sin\theta$$

where d is the atomic spacing between a cation and an anion in the crystal and n is a positive integer. [4]

For the crystals in this experiment, we attempted to measure their lattice constant, a, which is the spacing between adjacent unit cells in their crystal structures. Both LiF and KCl are cubic crystal, so their lattice constant is given by:

$$a = 2\,d\,.$$

This is also shown in Figure 2. Combining all the formulas, we have:

$$a = \frac{n\,\lambda}{\sin\theta}$$

where $n = 1, 2,$ etc., and θ is the incident angle such that constructive interference of the diffracted X-ray is observed for a certain wavelength, λ.

III. APPARATUS

We used a Tel-X-Ometer Model 580M as our X-ray spectrometer. It contains a hard vacuum, hot cathode X-ray tube. The tube has a copper target anode, and can be operated under an applied voltage of either 30 kV or 20 kV. High voltage is derived from a solid-state inverter circuit, followed by a Cockcroft-Walton type multiplier to provide a smooth DC output. The Tel-X-Ometer was also preset to operate at a current under 50 μA. [5] A multimeter was attached to the Tel-X-Ometer to monitor its operating current. The layout of the Tel-X-Ometer is shown in Figure 3. The crystal is mounted at the center and reflects the X-rays to a carriage. The carriage is fixed on a radial arm that can be slide and rotated. As the radial arm gets rotated, the crystal also rotates, but in a such way that the reflected beam is kept at an angle of 2θ with the incident beam. A table on the spectrometer allows us to read out the value of the angular displacement of the radial arm, or 2θ. Inside the carriage are two 3 mm beam collimators and a Geiger-Müller (G-M) tube.

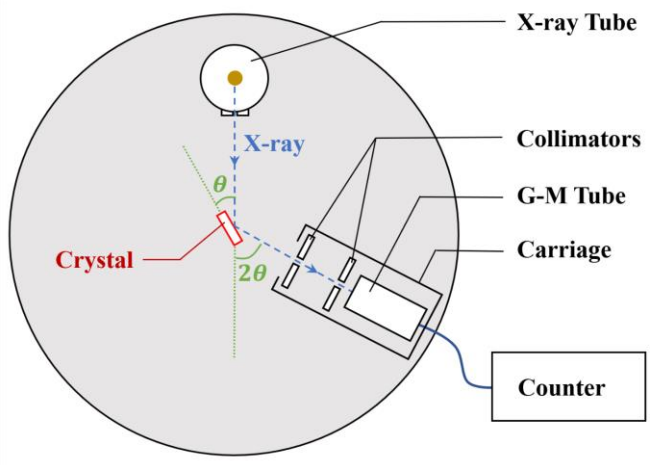

FIG. 3. Experimental Setup of the Tel-X-Ometer.

We used the G-M tube as our detector and a Nucleus Model 500 Scaler to record the number of particles detected by the G-M tube. The counter provides continuously variable regulated output voltages over a range of 0 to 2 kV. [6]

Besides, a fan is placed beneath the Tel-X-Ometer to cool the equipment and prevent it from getting overheat too quickly.

IV. EXPERIMENTAL PROCEDURE

We first stabilized the efficiency of the GM tube and the counter with respect to high voltage. To achieve this, we placed a radioactive source under the GM tube, and counted the radiation during a 30 seconds time interval at different voltage levels. We plotted the recorded count rate as a function of high voltage, ranging from 200 V to 1100 V, as shown in Fig. 4. At a low voltage, we saw nothing. At a high voltage (> 1 kV), we observed high count rate due to sparks erupted from the imperfections on the surface of the high voltage wire that travels down the center of the GM cylinder. At intermediate voltages, ranging from 300 V to 600 V, we observed a plateau in counting rate. We eventually settled at a working voltage of 450 V, which is around the middle of the plateau. The efficiency of the counter here should be stable over time relative to the inevitable changes in line voltage, the HV supply, temperature, humidity, air pressure, etc.

With the efficiency of our detector stabilized, we then setup the experiment as shown in Figure 3. We decided to first test on lithium fluoride (LiF). Before placing the crystal onto the Tel-X-Ometer, we polished the crystal to ensure that one side of the crystal was clear and smooth. That clear and smooth side would be the side that reflects the X-rays. We recorded the position of the two collimators and the G-M tube in the carriage. Then we turned on the Tel-X-Ometer and waited a minute for it to stabilize.

Then we started taking data. We first moved the carriage

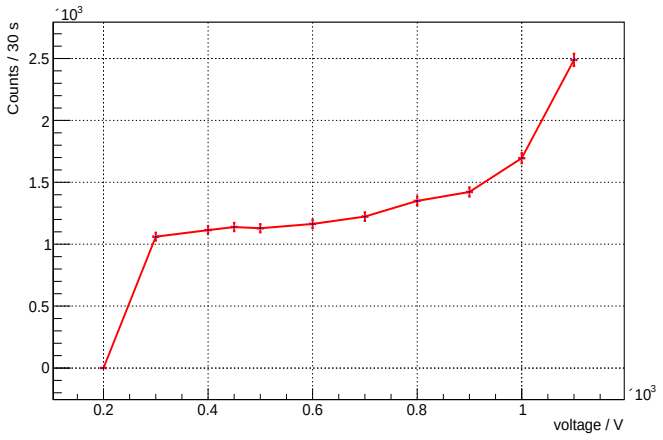

FIG. 4. Finding the plateau of the counter efficiency. The vertical axis is number of counts per 30 seconds, while the error bars represent sampling errors calculated by taking square root of counts.

to a certain angular position, recorded 2θ, and then started the counter and let it count for a fixed period of time (initially set to 1 minute but later changed to 30 seconds). We wrote down the counts before we repeat this measurement process for another value of 2θ. We increased the value of 2θ by 1 degree at a time.

As we took data, we also plot the counts on a computer in real time and monitored the change in count rates as 2θ changes. If a peak in the count rate showed up for a certain range of 2θ values, we would know that we were receiving constructive interference patterns formed by either the K_α or the K_β characteristic X-rays. To increase the resolution of the count rate peak, we would later repeat measurement for that range of 2θ and increased 2θ by only 0.25 degree between rounds of measurement.

After continuously operating for about 50 minutes, the filament in the X-ray tube typically got overheat and the number of electrons released declined. Once this happened, we had to paused the experiment, turned off the Tel-X-Ometer, and waited until it is cooled down so that we could resume our experiment.

We kept repeating this data taking process until we ran through the whole range of 2θ on the spectrometer table. We then replace the LiF crystal by a potassium chloride (KCl) crystal, and followed the same procedures as described above when we took measurements for KCl. Due to limit in time available, we didn't increase the peak count rate resolution for this crystal.

After taking data for both crystals, we started testing the magnitude of some systematic errors. We either replaced the X-ray tube by a new one, or switched the Tel-X-Ometer operating voltage from 30 kV to 20 kV, or replacing one 3 mm collimator by a 1 mm collimator, or using a counter voltage of 600 V instead of 450 V, or using a crystal that has an uneven and rough surface. We tested these systematic by using the LiF crystal and running a quick test with 2θ ranging from 37° to 49° where the two largest count rate peak were observed.

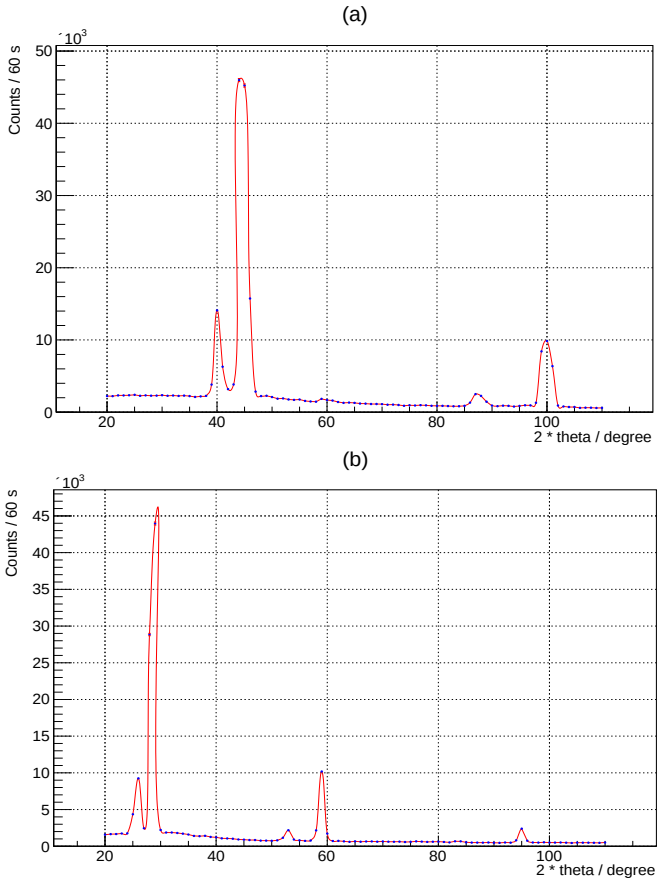

FIG. 5. Plots of counts per 30 seconds against 2θ. The vertical error bars represent sampling errors calculated by taking square root of counts. The horizontal error bars correspond to systematic errors in the measurement of 2θ. (a) Plot for LiF. (b) Plot for KCl. In (a) and (b), as 2θ increases, the $n = 1, K_\beta$ peak is first observed, followed by the $n = 1, K_\alpha$ peak, the $n = 2, K_\beta$ peak, and the $n = 2, K_\alpha$ peak. For KCl, the $n = 3, K_\alpha$ peak is also observed, but the $n = 3, K_\beta$ peak is not observed due to its low intensity. The non-peak areas in the plots are diffraction patterns corresponding to bremsstrahlung.

V. DATA ANALYSIS

Using CERN ROOT, we plot the count rates as a function of 2θ for both crystals as shown in Figure 5. From each graph, we read out the value of 2θ where the peaks are observed with corresponding systematic errors:

LiF, $n = 1, K_\beta$: $2\theta = 40.0° \pm 1.0°$
LiF, $n = 1, K_\alpha$: $2\theta = 44.5° \pm 1.5°$
LiF, $n = 2, K_\beta$: $2\theta = 87.5° \pm 1.5°$
LiF, $n = 2, K_\alpha$: $2\theta = 100.0° \pm 2.0°$

KCl, $n = 1, K_\beta$: $2\theta = 26.0° \pm 1.0°$
KCl, $n = 1, K_\alpha$: $2\theta = 28.5° \pm 1.5°$
KCl, $n = 2, K_\beta$: $2\theta = 53.0° \pm 1.0°$
KCl, $n = 2, K_\alpha$: $2\theta = 59.0° \pm 1.0°$
KCl, $n = 3, K_\alpha$: $2\theta = 95.0° \pm 1.0°$

The wavelengths of the characteristic X-rays produced are:

K_α: $\lambda = 154 \text{ pm} \pm 1 \text{ pm}$
K_β: $\lambda = 138 \text{ pm} \pm 1 \text{ pm}$

Using the formula,

$$a = \frac{n\lambda}{\sin\theta},$$

we calculate the implied lattice constant for each peak and propagate the errors accordingly:

LiF, $n = 1, K_\beta$: $a = 406 \text{ pm} \pm 11 \text{ pm}$
LiF, $n = 1, K_\alpha$: $a = 407 \text{ pm} \pm 14 \text{ pm}$
LiF, $n = 2, K_\beta$: $a = 399 \text{ pm} \pm 7 \text{ pm}$
LiF, $n = 2, K_\alpha$: $a = 402 \text{ pm} \pm 9 \text{ pm}$

KCl, $n = 1, K_\beta$: $a = 614 \text{ pm} \pm 24 \text{ pm}$
KCl, $n = 1, K_\alpha$: $a = 626 \text{ pm} \pm 33 \text{ pm}$
KCl, $n = 2, K_\beta$: $a = 619 \text{ pm} \pm 13 \text{ pm}$
KCl, $n = 2, K_\alpha$: $a = 626 \text{ pm} \pm 11 \text{ pm}$
KCl, $n = 3, K_\alpha$: $a = 627 \text{ pm} \pm 8 \text{ pm}$

Then by taking the average we derive the final results:

LiF: $a = 403\ \text{pm} \pm 5\ \text{pm}\ (1.2\%)$

KCl: $a = 622\ \text{pm} \pm 9\ \text{pm}\ (1.4\%)$

The accepted lattice constants for these two crystals are:

LiF: $a = 403.5\ \text{pm}$

KCl: $a = 629.2\ \text{pm}$

Thus, percentage deviations of our results from the accepted values are 0.2% and 1.2% for LiF and KCl, respectively.

The error bars in our results represent systematic errors and they are mostly errors in angular measurement of 2θ. Multiple factors contribute to this error. For example, the crystal may not be perfectly mounted on the Tel-X-Ometer to match the θ table on the spectrometer. For another example, the resolution of our measurement is limited by the width of the beam collimator. By replacing one 3 mm collimator by a 1 mm collimator, we observed sharper peaks in the count rate plots, indicating an increase in resolution.

Having an uneven crystal surface also reduced the peak resolution as we observed wider peaks in our systematic error tests. Having an uneven surface means that the X-ray are scattered at different angles more randomly, reducing the amount of constructive interference at certain angles.

We also tested some other systematic errors, and found that errors caused by variation in Tel-X-Ometer operating voltage and errors caused by variation in counter voltage were trivial.

Our experiment ran for about 4 weeks, and over the course of this experiment, we observed that the operating current of the X-ray tube slowly increased over time despite days of cooling down. A higher current results in more electrons being emitted and a higher count rate recorded by the counter. Besides, the resolution of the peak also gets lower when the current is high. We confirmed these effects when we replaced the X-ray tube by a new one, which greatly reduced the operating current from around $50\ \mu\text{A}$ to around $30\ \mu\text{A}$. Since our rounds of measurement process usually took hours, this slowly increase in current over time introduced a systematic error, especially when we wanted to compare count rates measured at the same 2θ but under different conditions.

VI. CONCLUSION

Using an X-ray spectrometer to create X-ray diffraction patterns, we were able to investigate the crystal structures of lithium fluoride (LiF) and potassium chloride (KCl). Using Bragg's law, we derived the lattice constant of LiF to be $403\ \text{pm} \pm 5\ \text{pm}\ (1.2\%)$, and derived the lattice constant of KCl to be $622\ \text{pm} \pm 9\ \text{pm}\ (1.4\%)$. The accepted values of lattice constant fall within the range of our results.

VII. ACKNOWLEDGEMENTS

The authors express sincere appreciation to Yaokun Situ, Lawrence R. Sulak, and Daniel Arcaro of Boston University for sharing their valuable experience and guidance.

[1] R. Novelize, *Squire's Fundamentals of Radiology* (Harvard University Press, Cambridge, 1997).

[2] S. G. Tomlin, *Australian Dictionary of Biography* (Australian National University, Canberra, 1979).

[3] S. Lemarc, https://www.slideshare.net/slemarc/investigation-of-crystal-structures-and-xray-diffraction-sultan-lemarc.

[4] R. W. James, *The Optical Principles of The Diffraction of X-Rays* (G. Bell and Sons Ltd., London, 1962).

[5] See operation manual at http://www.phys.utk.edu/labs/modphys/TEL-X-OMETER%20580%20Manual.pdf.

[6] See operation manual at http://www.fen.bilkent.edu.tr/~mb/phys230/manuals/exp8_nuclear_spectroscopy.pdf.